JOC The Journal of Organic Chemistry

Article

pubs.acs.org/joc

Biomimetic One-Pot Route to Acridine Epoxides

Margarida Linhares, Susana L. H. Rebelo,* Krzysztof Biernacki, Alexandre L. Magalhães, and Cristina Freire

REQUIMTE, Departamento de Química e Bioquímica, Faculdade de Ciências, Universidade do Porto, Rua do Campo Alegre, 4169-007 Porto, Portugal

Supporting Information

ABSTRACT: The first direct epoxidation of acridine on the edge positions is reported. The reaction proceeds under mild conditions using a biomimetic catalytic system based on a Mn(III) porphyrin. The successive oxyfunctionalization to mono-, di-, and tetraepoxy derivatives is accomplished using hydrogen peroxide as a green oxidant at room temperature. Computed optimized geometries showed only slight shifts to the base planarity upon dearomatization by epoxidation, which is an important feature for DNA intercalation and bioactivity. NMR studies and comparison with theoretical values allowed the assignment of the stereochemistry of the *anti*- and *syn*-diepoxy and -tetraepoxy derivatives as well as compounds resulting from epoxide ring opening, exemplified by epoxydiol. The diepoxide is formed in an *anti*:*syn* ratio of ~4, and the attack by nucleophiles, exemplified by ethylaniline, occurs selectively and with full conversion, using a microwave process with acetonitrile reflux for 10 min. Finally, studies of the electrostatic potential allowed the mechanisms of the formation of 4-hydroxyacridine and the regioselective reaction of diepoxyacridine with nucleophiles to be rationalized.

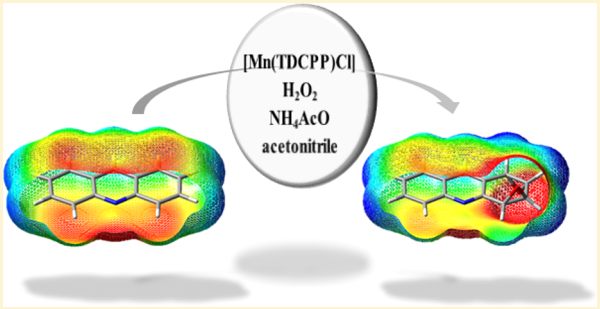

INTRODUCTION

Acridine derivatives are an important class of bioactive compounds that have been widely studied for their antibacterial[1] and antimalarial[2] activities, while the more recent research has mainly focused on their use as potential therapeutic agents for cancer[3−5] and Alzheimers's disease.[6] A key feature of these molecules is the planar base structure, which allows strong but reversible intercalation into DNA chains between nitrogen bases[7] and inhibition of topoisomerase enzymes.[8] More recently, the antibacterial activity has been ascribed to their activity as amphiphilic membrane disruptors.[9] The most recent studies considered platinum−acridine hybrid agents showing synergistic metalating−intercaling properties and very promising activity for the treatment of chemoresistant cancers.[10,11] The understanding of the mode of action of these compounds and the existence of different biological targets has stimulated the synthesis of new acridine derivatives. In addition, substituted acridine chromophores have found extensive applications as luminescent probes, essentially chemiluminescent and fluorescent.[12−14]

Despite the many studies developed for the preparation of compounds based on the acridine structure, direct substitution on the acridine backbone occurs only at the most reactive *meso* position (position 9, opposite to the nitrogen atom; see Scheme 1 for atom numbering) or by nucleophilic attack at the central *N*-pyridyl site.[15] Consequently, acridines carrying substituents on the peripheral aromatic rings commonly result from addition and cyclization reactions of lower-mass compounds. These type of reactions often require several steps with the formation of significant amounts of secondary products and the demand for high temperatures and long reaction times in the individual steps.[16]

Cytochrome P450 enzymes play a key role in metabolic pathways, as they are responsible for a wide range of selective oxygenation reactions,[17] and they promote the activation of green oxidants such as molecular oxygen and hydrogen peroxide.[18,19] One of the most unusual reactions mediated by P450 is the direct epoxidation of aromatic rings, which is ultimately associated with the mutagenic properties of polycyclic aromatic compounds due to the reaction of the epoxide rings with DNA bases.[20,21]

Since aromatic epoxidation by chemical systems is not common, the development of efficient pathways to new and potential useful derivatives can be inspired by biomimetic processes. After epoxidation at peripheral positions and convenient derivatization of the epoxides, several stable acridine derivatives can be obtained. These compounds have very promising bioactivities[22,23] due to the possibility of intercalation and reversible binding to DNA.

On the basis of the prosthetic center of cytochrome P450, an iron(III) protoporphyrin IX with a cysteine as the axial ligand, synthetic metalloporphyrins carrying electron-withdrawing substituents have been increasingly and successfully used in the oxidation of various organic substrates. Novel processes have been described for the oxidation of, e.g., alkenes,[24] inert

Received: October 14, 2014
Published: November 22, 2014

   dx.doi.org/10.1021/jo5023525 | J. Org. Chem. 2015, 80, 281−289

Scheme 1. Acridine Derivatives Obtained by Biomimetic Oxidation in the Presence of [Mn(TDCPP)Cl] and H_2O_2

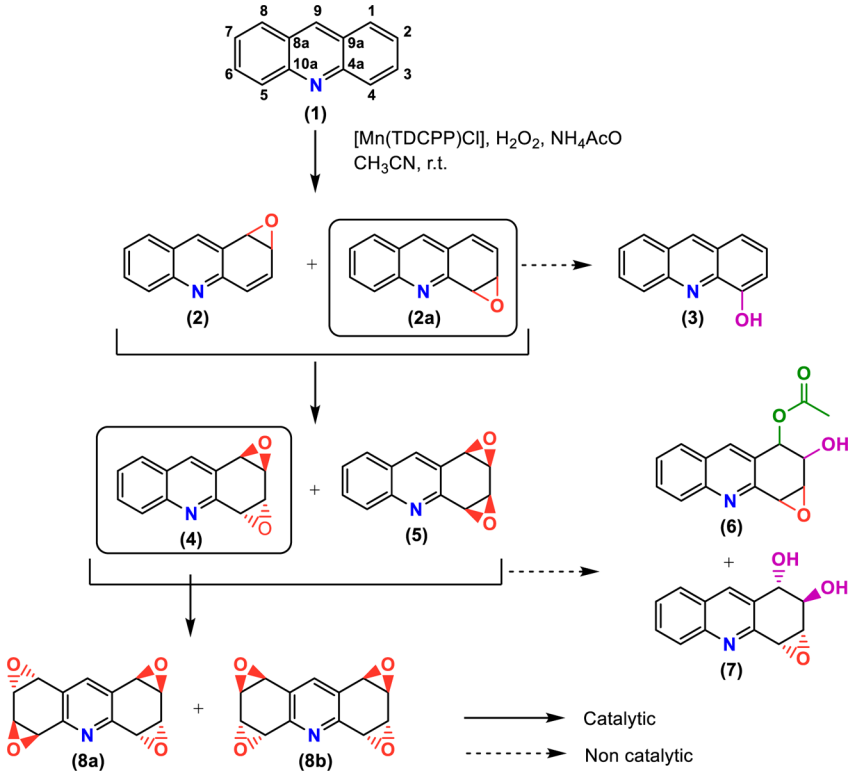

Table 1. Effect of Reaction Time and Amount of Oxidant Added on the Formation of Acridine Derivatives

		product yields (%)[a]							
conditions[b]	conversion (%)	2	3	4	5	6	7	8a	8b
A: 1 h, S:C = 300, 2 equiv of H_2O_2(aq)	77	27	3	38	9	–	–	–	–
B: 3 h, S:C = 300, 6 equiv of UHP	100	–	–	70	17	5	8	–	–
C: 15.5 h, S:C = 100, 31 equiv of UHP	100	–	–	49	11	8	11	15	6

[a]The numbers correspond to the structures in Scheme 1. [b]S:C = substrate:catalyst ratio.

alkane C−H bonds,[25] sulfur compounds,[26−28] and aromatics.[29] These processes are particularly relevant for the urgent replacement of stoichiometric oxidants.

The manganese(III) porphyrin catalyst chloro[5,10,15,20-tetrakis(2,6- dichlorophenyl)porphyrinato]manganese(III), [Mn(TDCPP)Cl] (see the Supporting Information for its structure), showed a singular ability toward the direct epoxidation of the peripheral positions of linear polycyclic aromatic structures (acenes) at room temperature.[30] When hydrogen peroxide was used as the oxidant, the presence of an aprotic solvent and a cocatalyst was necessary.[31] In the present work, a related biomimetic system was applied to synthesize acridine mono-, di-, and tetraepoxides under mild conditions. The studies considered theoretical calculations to corroborate structure and reactivity insights.

RESULTS AND DISCUSSION

Synthesis of Epoxyacridine Derivatives. The oxidation of acridine in the presence of the metalloporphyrin catalyst [Mn(TDCPP)Cl] and hydrogen peroxide using acetonitrile as the solvent and ammonium acetate as an inorganic cost-effective cocatalyst[29] afforded the progressive dearomatization and epoxidation of the azatricyclic structure (Scheme 1). For each product, only one possible enantiomer is shown. The reaction was repeated using different reaction times (corresponding to different total amounts of oxidant added) and various substrate:catalyst ratios (S:C), as described in Table 1.

Upon 1 h of reaction (Table 1, condition A), the substrate conversion was 77% and the most abundant products obtained were 1:2-epoxy-1,2-dihydroacridine (**2**) and *anti*-1:2,3:4-diepoxy-1,2,3,4-tetrahydroacridine (**4**) in 27% and 38% yield, respectively. Minor products were *syn*-1:2,3:4-diepoxy-1,2,3,4-tetrahydroacridine (**5**) in 9% yield and a hydroxylated compound, 4-hydroxyacridine (**3**), in 3% yield. When the reaction time was increased to 3 h and the hydrogen peroxide adduct with urea (UHP) was used as an anhydrous oxidant form (Table 1, condition B), the catalytic reaction afforded total substrate conversion and the mono-oxygenated products were not isolated. The yields of diepoxides **4** and **5** almost doubled to 70% and 17%, respectively. In addition, the reaction afforded small amounts of two products resulting from epoxide ring opening, compound **6** from ring opening by acetate ion from the cocatalyst and epoxydiol derivative **7** from ring opening by water present in the reaction mixture. Extending the reaction time to 15.5 h and reducing the S:C from 300 to 100 (Table 1, condition C) afforded tetraepoxy derivatives **8a** and **8b**, although in low yields of 15% and 6%, respectively. Concomitantly, the amounts of compounds **6** and **7** increased at the expense of decreases in the yields of diepoxyacridines.

dx.doi.org/10.1021/jo5023525 | J. Org. Chem. 2015, 80, 281−289

Under all of the conditions of Table 1 (A–C), the *anti*:*syn* (**4**:**5**) ratio of the produced diepoxides was always ~4.2, indicating the diastereoselective condition of the substrate approach to the large catalytic active species in the second epoxidation.

The introduction of the third and fourth epoxide groups is less efficient compared with the first and second epoxidations, since the aromatic character increases in going from three to two fused linear aromatic rings, in accordance with Clar's rule. In fact, when *anti* diepoxide **4** was used as the substrate for a catalytic oxidation under the same conditions as acridine (condition B), after 6 h of reaction time the conversion was only 47% and the isolated yield of tetraepoxides was 20%, while compounds **6** and **7** resulting from epoxide ring opening were isolated in yields of 14% and 13%, respectively.

Planarity of the Structures. Density functional theory (DFT) calculations at the B3LYP level afforded the lowest-energy structures of compounds **2**, **3**, **4**, and **8a**, as depicted in Figure 1. Other structures are shown in the Supporting Information. The tricyclic backbone in compound **3** has a planar structure, while those in compounds **2**, **4**, and **8a** are slightly distorted from a planar geometry; the epoxide rings are above or below the plane. These results evidence that upon loss of aromaticity the resulting cyclohexene rings are far from the expected boat/chair conformations. The dihedral angles listed in Table S2 in the Supporting Information are distributed around |0°| or |180°|, confirming that the backbones of the mono-, di-, and tetraepoxides of acridine are essentially planar structures.

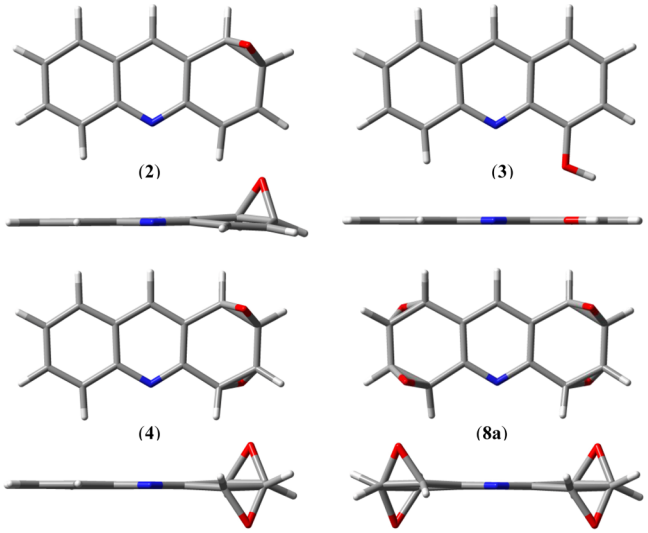

Figure 1. Optimized structures (top and side views) of acridine derivatives **2**, **3**, **4**, and **8a** obtained at the B3LYP/6-31G(d,p) level of calculation.

In this series of compounds, 1:2-epoxyacridine (**2**) shows the highest distortions to planarity. The same base planar structures are observed for compounds **5** and **8b** (see the Supporting Information). The maintenance of a nearly planar alignment for the tricyclic backbone reveals an important feature of these molecules that allows the possibility of DNA intercalation.

Stereochemical Assignments. *anti- and syn-Diepoxides.* The aliphatic zones of the ^{1}H NMR spectra of compounds **4** and **5** (Figure 2) show a clear difference in the shape and shift of the proton signals for the two diepoxyacridines. This highlights the symmetry factors (bearing in mind the planarity of the structures as previously demonstrated) and the inductive/anisotropic effects of the two oxygen atoms being on opposite sides or on the same side of the tricyclic base plane, thus attenuating or reinforcing the proton shielding. A differentiation between the two diastereoisomers based on detailed analysis of the ^{1}H and ^{13}C spectra is provided in the Supporting Information.

On the other hand, 2D NMR studies could not distinguish between the stereochemistries of compounds **4** and **5**: the NOESY spectra of both showed a correlation between H1 and H9 (see the Supporting Information), and consequently, the definitive identification of the *anti*- and *syn*- diepoxyacridines could be interchanged. As a further resource, DFT simulations of ^{1}H and ^{13}C NMR shifts were used to confirm the assignments of the two structures.

A graphical comparison of the theoretical ^{1}H chemical shifts with the experimental values for compounds **4** and **5** is shown in Figure 3, which includes an expansion of the most significant aliphatic region. The mean absolute deviation $\bar{D}$ (see the definition in the Experimental Section and the tables of all data in the Supporting Information) was used as a comparison parameter, with the acridine molecule ($\bar{D}$ = 0.03) used as the reference. The values of $\bar{D}$ obtained from the comparison between the experimental ^{1}H NMR shifts of compound **4** and the theoretical ^{1}H NMR shifts of the *anti* and *syn* isomers were 0.04 and 0.10, respectively, while the values obtained from the comparison of compound **5** and the theoretical shifts of the *anti* and *syn* isomers were 0.13 and 0.03, respectively. In accordance with these results, it was possible to assign compound **4** as *anti* and compound **5** as *syn*.

Tetraepoxides. Tetraepoxyacridine has six possible diastereoisomers, although only two of these isomers were isolated. The stereochemistry assignment of the isolated tetraepoxides was based on the combination of experimental NMR studies and DFT calculations. The experimental ^{1}H NMR shifts of compounds **8a** and **8b** were compared with the theoretical

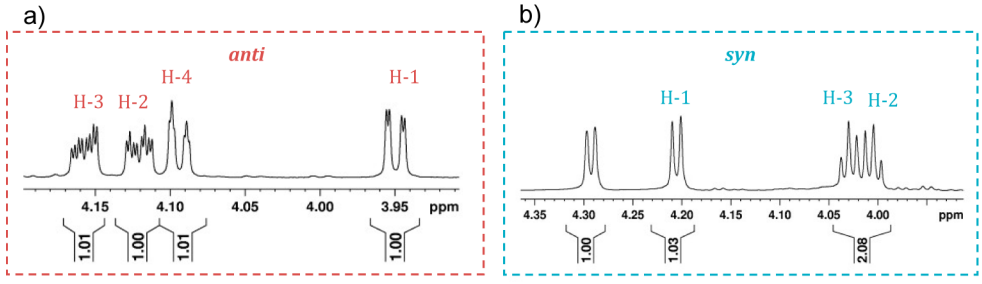

Figure 2. Aliphatic zone of the ^{1}H NMR spectra of (a) *anti*-diepoxyacridine (**4**) and (b) *syn*-diepoxyacridine (**5**).

dx.doi.org/10.1021/jo5023525 | J. Org. Chem. 2015, 80, 281–289

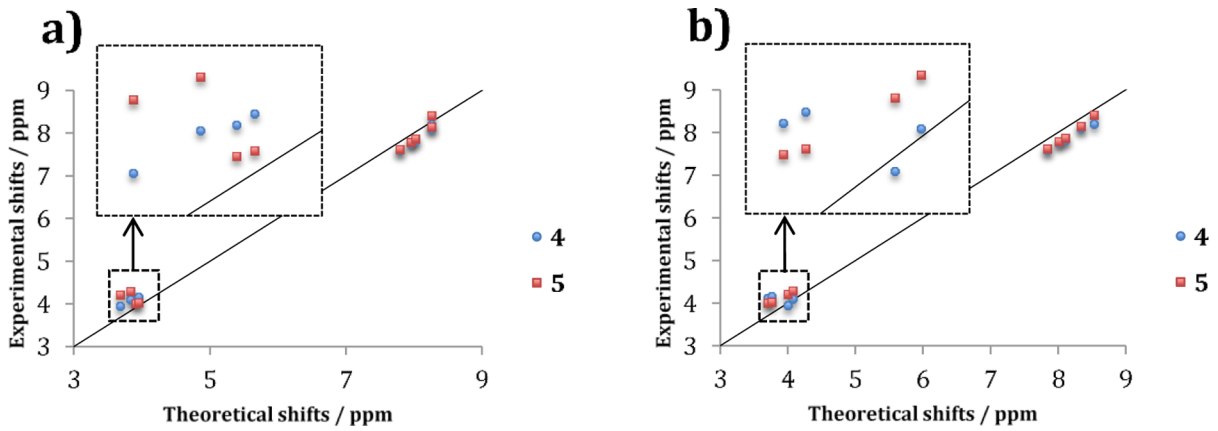

Figure 3. Comparison of experimental ^{1}H NMR shifts of compounds **4** and **5** with the theoretical values obtained for (a) *anti*-diepoxyacridine and (b) *syn*-diepoxyacridine.

shifts obtained by DFT calculations for the six possible diastereoisomers. Table 2 shows the values of $\bar{D}$ obtained for all the comparisons: the *anti,anti* stereoisomers are classified as aa1 and aa2, the *syn,anti* isomers as sa1 and sa2, and the *syn,syn* isomers as ss1 and ss2. Analysis of all of the mean absolute error deviations indicated that compounds **8a** and **8b** are the two *anti,anti* isomers (aa1 and aa2) (Scheme 1) and not the *anti,syn* or *syn,syn* isomers.

Table 2. Values of the Mean Absolute Deviation ($\bar{D}$) between the Experimental and Theoretical Chemical Shifts in the ^{1}H NMR Spectra of Tetraepoxides

	$\bar{D}$					
	aa1	aa2	sa1	sa2	ss1	ss2
8a	0.05	0.05	0.08	0.08	0.11	0.12
8b	0.06	0.05	0.08	0.08	0.12	0.13

Further differentiation between the two *anti,anti* structures and attribution of the stereochemistry of compounds **8a** and **8b** considered the analysis of the full ^{1}H NMR spectrum of a mixture of these two isomers (Figure 4). The nearly planar structures obtained for the lowest-energy conformations by DFT justify the molecular symmetry perceived in the spectrum. In the aliphatic zone, each signal corresponds to two protons, while in the aromatic region only the singlet attributed to the proton H9 appears, at 7.76 ppm for **8a** and 7.75 ppm for **8b**. The positioning of the epoxides at positions 1:2 and 7:8 on opposite sides or the same side of the backbone structure can cause a reduction or reinforcement of the inductive and anisotropic effects, respectively, similar to the effect observed for the *anti*- and *syn*-diepoxides **4** and **5** though in this case with less intensity. Thus, it can be justified that H1 and H8 are more protected and the corresponding signals are observed at lower frequencies in the isomer **8a** than in the isomer **8b**, and the same applies for protons H4 and H5.

On the other hand, a greater yield of compound **8a** would be expected, since this isomer will be obtained as two enantiomers, increasing the likelihood of its formation relative to compound **8b**.

Epoxydiol. The assignment of the stereochemistry of compound **7** considered the optimized structures of possible diastereoisomers and a comparison of theoretical ^{1}H NMR shifts with experimental ones using the $\bar{D}$ value as the comparison parameter.

Nucleophic attack by a water molecule at C1 can lead to different isomers, as shown in Figure 5. Structures **a** and **b** result from epoxide ring opening of *anti*- diepoxyacridine **4** in a *trans* faction; structures **c** and **d** result from epoxide ring opening of *syn*-diepoxyacridine **5** in a *trans* faction; and

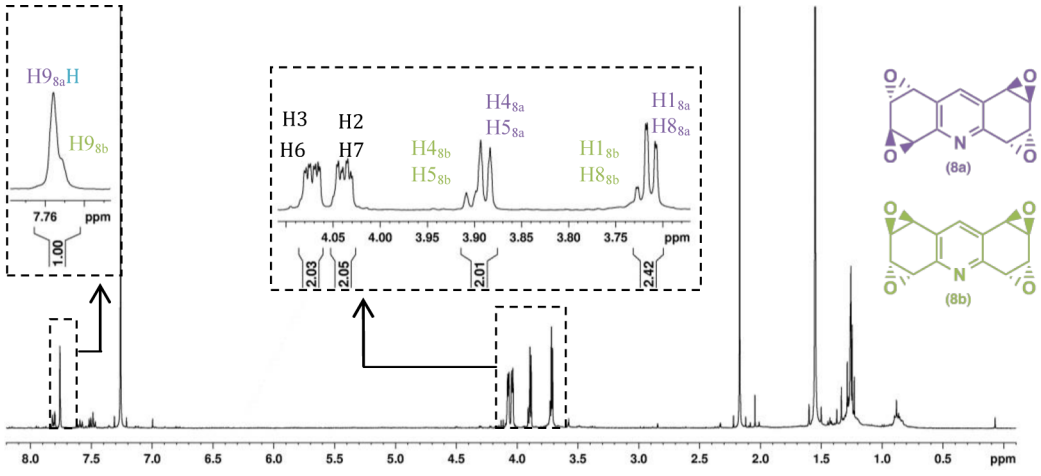

Figure 4. ^{1}H NMR spectrum of a mixture of *anti,anti*-tetraepoxides **8a** and **8b**.

dx.doi.org/10.1021/jo5023525 | J. Org. Chem. 2015, 80, 281−289

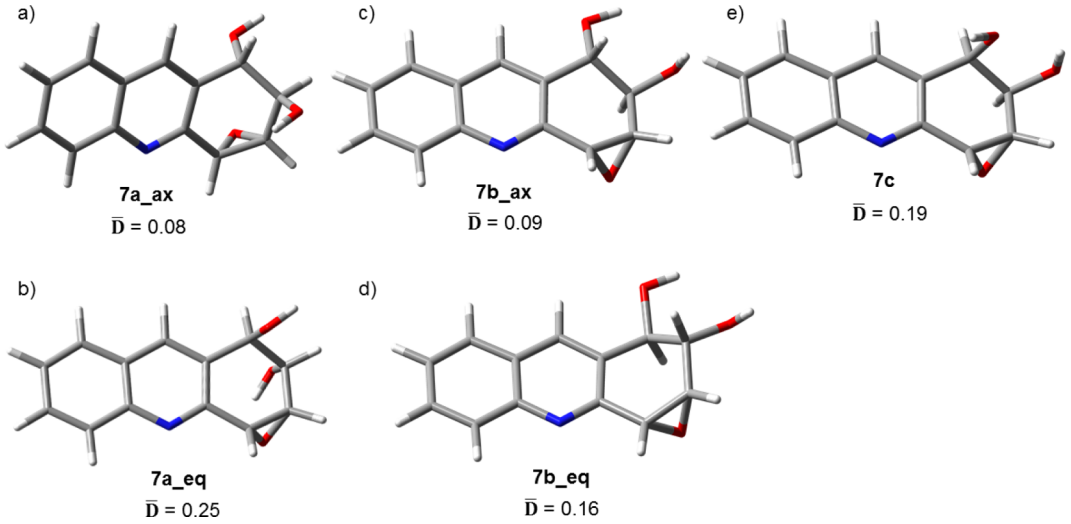

Figure 5. Optimized structures of possible stereoisomers of compound 7 obtained at the B3LYP/6-31G(d,p) level of calculation.

structure **e** results from epoxide ring opening of *anti*-diepoxyacridine **4** in a *cis* faction. All of these structures, after optimization, showed conformations at the 1,2-position that approximate boat/chair with significant shifts to planarity. Consequently, the possible conformations considered the positioning of the hydroxyl groups at axial positions (structures **a** and **c**) or at equatorial positions (structures **b** and **d**).

The structures **7a_ax** and **7b_ax** have the lowest $\bar{D}$ values (0.08 and 0.09, respectively), while the other structures show significantly higher values. Thus, it is possible to assign a *trans*-diol structure with the hydroxyl groups in axial positions (structure **a** or **c**) to compound **7**. However, the slightly lower $\bar{D}$ value for compound **7a_ax** and the more abundant production of the *anti*-diepoxyacridine (the precursor of **7a_ax**) relative to the *syn* isomer confirm the assignment of the structure **7a_ax** to compound **7**. Its enantiomer (**7a_ax′**) also gave a $\bar{D}$ value of 0.08 (see the Supporting Information). Other possible structures, namely, considering the diol moiety to be hydrogen-bonded with an external water molecule, all gave considerably higher $\bar{D}$ values (see the Supporting Information). The total electronic energies of the optimized structures are also collected in Table S16 in the Supporting Information. However, the values are too similar to allow differentiation among the isomeric structures.

Regioselective Monooxygenation: Aromatic Hydroxylation versus Epoxidation. The ^{1}H−^{1}H NMR NOESY spectrum of monoepoxide **2** shows a correlation between H1 and H9, confirming the regioselective epoxidation at the 1:2 position and not at the 3:4 position. On the other hand, 4-hydroxyacridine (**3**) was the only hydroxylated product isolated from the reaction mixture.[16]

Aromatic hydroxylation by cytochrome P450 enzymes and metalloporphyrin biomimetic models has been extensively investigated over the past decades, but the related mechanism is still controversial.[32] In particular, an open discussion remains on the possibility of initial epoxidation of the aromatic ring with further rearrangement (Scheme 2, path A) or instead electrophilic attack on the aromatic π system to produce a tetrahedral radical or cationic σ complex (Scheme 2, path B for a cationic σ complex). While the first path was initially proposed in the presence of cytochrome P450 active species (so-called compound I),[33] the second path was proposed to occur for iron porphyrin models.[34,35] A recent study also

Scheme 2. Possible Pathways for the Aromatic Hydroxylation Reaction Catalyzed by Metalloporphyrins

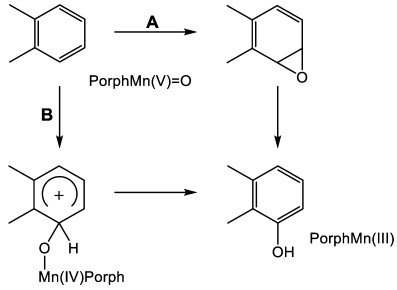

provided evidence that both pathways can occur, depending on the reaction conditions.[36]

The formation of **3** as the only hydroxylated product could result from both mechanisms, highlighted by the fact that 3:4-monoepoxide (compound **2a**) was not found amid the reaction products. However, on the basis of the map of the potential energy surface and the partial charges for acridine (**1**) (Figure 6a,b) it is not possible to justify the exclusive hydroxylation on position 4 by path B. On the other hand, the electrostatic potential (ESP) values obtained for the two monoepoxide isomers, 1:2-epoxyacridine (**2**) and 3:4-epoxyacridine (**2a**) (Figure 6c,d) reveal that the difference in the charges of carbons C3 and C4 in **2a** ($|\Delta|_{3,4} = 0.209e$) is significantly larger than that between carbons C1 and C2 of **2** ($|\Delta|_{1,2} = 0.058e$). These results can justify a greater tendency of **2a** to open relative to compound **2**, leading to the complete conversion of compound **2a** into the 4-hydroxylated derivative (compound **3**).

Furthermore, the map for acridine (Figure 6a) evidences a more uniform distribution of electron density between carbons C1 and C2 than between carbons C3 and C4, where the electron density is more concentrated on C4. This justifies preferential epoxidation by attack on the π system at the 1:2 position instead of the 3:4 position and the higher yield obtained for compound **2** (27%) relative to compound **3** (3%).

As a confirmation, analysis of the ^{1}H NMR spectrum of the total reaction mixture (see the Supporting Information) did not show the signals attributed to 4-hydroxyacridine (**3**), while signals similar to those of 1:2-epoxyacridine (**2**) were detected

dx.doi.org/10.1021/jo5023525 | J. Org. Chem. 2015, 80, 281−289

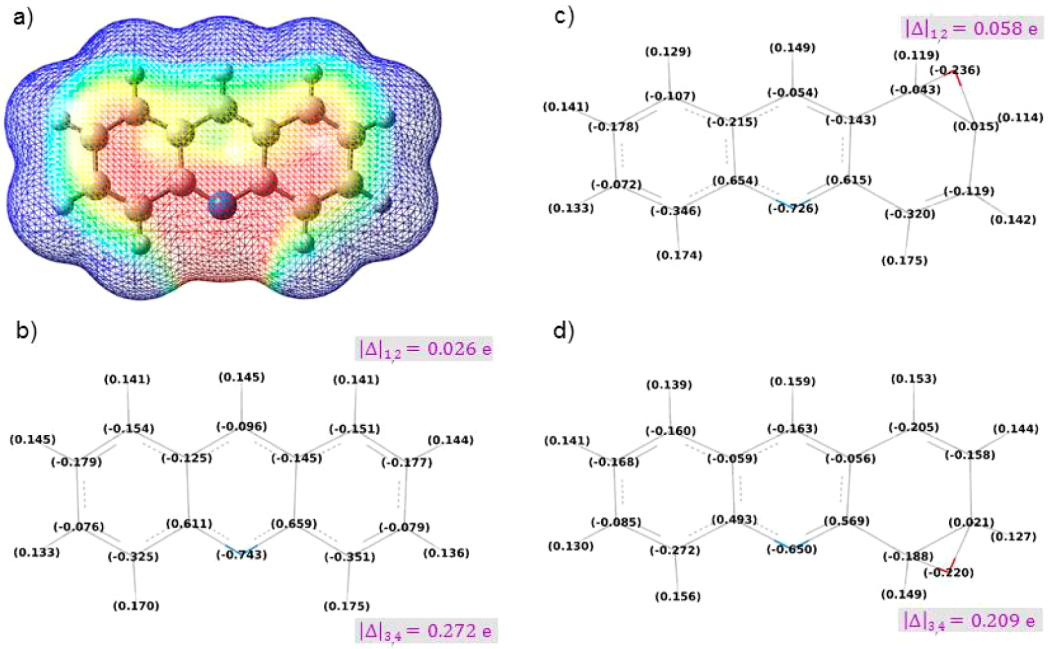

Figure 6. (a) Electrostatic potential map defined on the 0.0004 e/a_0^3 isodensity surface for acridine (**1**) and (b–d) ESP fitting charges of each atom for (b) acridine (**1**), (c) 1:2-epoxyacridine (**2**), and (d) 3:4-epoxyacridine (**2a**).

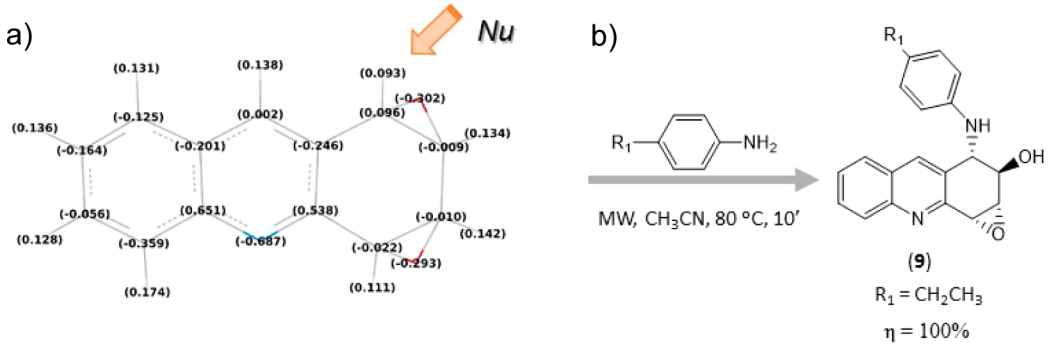

Figure 7. (a) ESP fitting charges of each atom in compound **4**. (b) Selective attack by nucleophiles at position 1.

[6.88 ppm (dd), 6.53 ppm (dd), and 4.74 ppm (d)]. These can be ascribed to the presence of 3:4-epoxyacridine (**2a**) in the mixture, though it is easily converted to compound **3** during workup of the reaction mixture. In addition, there was no trace of compound **3** or derivatives among the products of the reactions performed under conditions B and C, indicating that under those conditions the reaction went on with the formation of a second epoxide ring on both compounds **2** and **2a**, leading to diepoxide derivatives. Consequently, the possibility of direct hydroxylation on the aromatic ring of acridine by the active species of [Mn(TDCPP)Cl] finds itself excluded.

Selective Attack by Nucleophiles. The opening of epoxide rings by nucleophiles can lead to new, easily obtainable, and relevant acridine derivatives. Figure 7a shows the charge assigned to each of the atoms in compound **4**. It can be observed that C1 has a positive charge of 0.096*e*, indicating that this carbon will be the only one to undergo nucleophilic attack, which therefore occurs in a selective way. Regioselective epoxide ring openings by the acetate ion and by water present in the reaction mixture led to trifunctional derivatives **6** and **7**, respectively. These compounds carry one epoxide ring, one hydroxyl group, and a new functional group arising from the nucleophile. The cloud of electron density shown in the Supporting Information also corroborates that the epoxide ring opening occurs in a *trans* fashion, in accordance with the structure assigned to compound **7**.

The reaction between *anti*-diepoxyacridine (**4**) and 4-ethylaniline was carried out as a model reaction for the opening of the isolated epoxidized compounds in order to form new functionalized derivatives (Figure 7b). The reaction was performed in a microwave reactor using acetonitrile as the solvent with heating at 80 °C for 10 min. Compound **4** was completely and selectively converted to the new derivative 1-(4′-ethylphenylamino)-3:4-epoxy-2-hydroxyacridine (**9**).

■ CONCLUSIONS

In view of the small number of reactions described for the direct functionalization of acridine at the peripheral positions, particularly in regard to oxidation reactions, the herein described biomimetic procedure leads to a wide range of acridine derivatives by new and simpler (essentially "greener") synthetic pathways.

The acridine epoxides can be directly studied in mutagenic reactions, exploring the planarity and thereby the possible

dx.doi.org/10.1021/jo5023525 | *J. Org. Chem.* 2015, 80, 281–289

intercalation in the DNA structure. On the other hand, they can be easily transformed onto a variety of stable derivatives that have high potentiality in the prevention of tumor development. Thus, the new compounds may boost new synthesis routes for obtaining anticancer and antipathogenic drugs or even new drugs with greater biological selectivity.

Furthermore, compounds **6**, **7**, and **9** that result from epoxide ring opening can be tested in metal coordination. These compounds, alongside compound **3**, can find applications in sensing and novel chemotherapeutics based on DNA metalating−intercalating hybrids.

EXPERIMENTAL SECTION

General Experimental Information. All purchased chemicals were used as received. Thin-layer chromatography (TLC) was performed on plates of silica gel 60 F_{254} and visualized by UV irradiation. NMR experiments were conducted at frequencies of 400.15 and 100.63 MHz for ^{1}H and ^{13}C spectra, respectively, using $CDCl_3$ (99.8% D) as the solvent and $CHCl_3$ as the reference (δ = 7.260 ppm for ^{1}H NMR and 77.16 ppm for ^{13}C NMR). Bidimensional NMR experiments included ^{1}H−^{1}H COSY and NOESY and ^{13}C−^{1}H HSQC, HMBC, and APT. NMR data are reported as follows: chemical shift in parts per million (multiplicity, coupling constants in hertz, integration). Multiplicities are abbreviated as follows: s = singlet, d = doublet, t = triplet, m = multiplet, dd = doublet of doublets, dt = doublet of triplets, ddd = doublet of doublets of doublets. Mass spectra of the reaction products were recorded with electron impact ionization (EI) at 70 eV, and high-resolution mass spectra of reaction products and the catalyst were obtained with electrospray ionization in positive mode (ESI^+) using an LTQ Orbitrap XL mass spectrometer. A CEM Discover microwave synthesizer with maximum power level of 300 W and an external infrared temperature sensor was employed for the microwave-assisted experiments.

The metalloporphyrin catalyst chloro[5,10,15,20-tetrakis(2,6-dichlorophenyl)porphyrinato]manganese(III), [Mn(TDCPP)Cl], was prepared according to the procedure described in the literature.[29] HRMS (ES) *m/z*: calcd for $C_{44}H_{20}Cl_8MnN_4$ $[M - Cl]^+$ 938.85767, found 938.86046; the experimental isotopic pattern matched the theoretical one.

Acridine Oxidation. *General Procedure.* Acridine (0.3 mmol, 53.7 mg), the appropriate amount of the [Mn(TDCPP)Cl] catalyst (1 μmol, 1 mg or 3 μmol, 3 mg), and ammonium acetate (0.4 mmol, 30 mg) were dissolved in 4 mL of CH_3CN. Aliquots of hydrogen peroxide were added at a rate of 2 molar equiv/h under magnetic stirring at room temperature (~20 °C). The reactions were monitored by TLC using a solution of chloroform with 10% methanol as the eluent.

Reaction conditions A−C were tested, in which the reaction time (and consequently the final amount of oxidant added) and also the form of the oxidant (an aqueous solution (30% w/w) or an urea adduct (UHP)) were varied; under condition C, a lower substrate:catalyst ratio (S:C) was used.

Condition A. To the reaction mixture with 1 mg of catalyst (S:C = 300) was added an aqueous solution of H_2O_2 (30% w/w) diluted in acetonitrile (1:4) over 1 h (0.15 mmol of H_2O_2 each 15 min) for a total of 2 molar equiv relative to the substrate. The final products were isolated by preparative TLC with a 1:1 $CHCl_3/CH_3COOEt$ mixture as the eluent.

Condition B. To the reaction mixture with 1 mg of catalyst (S:C = 300) was added UHP progressively in portions of 0.15 mmol (14 mg) every 15 min for 3 h to attain a total of 6 molar equiv relative to the substrate. The final products were isolated by TLC: a first separation used as the eluent $CHCl_3$ containing 1% MeOH for less polar compounds (**1**, **4**, and **5**), and a second separation used $CHCl_3$ containing 5% MeOH for the isolation of more polar compounds (**6** and **7**).

Condition C. To the reaction mixture with 3 mg of catalyst (S:C = 100) was added UHP progressively in portions of 0.15 mmol (14 mg) every 15 min to attain a total of 31 molar equiv relative to the substrate. The products were isolated by a series of preparative TLC separations using successively the following eluents: chloroform containing 5% methanol; ethyl acetate and chloroform (1:3); and ethyl acetate and chloroform (1:1).

For the ^{1}H NMR analysis of the total reaction mixture, the solvent was evaporated and the mixture was dissolved in $CDCl_3$. The conversion was based on the mass of recovered substrate, and both isolated yields and yields based on the ^{1}H NMR spectrum of the total reaction mixture were calculated.

*Oxidation of anti-Diepoxyacridine (**4**).* The reaction followed the general procedure for acridine oxidation, and to the reaction mixture with 1 mg of catalyst (S:C = 300) was added UHP in portions of 0.15 mmol (14 mg) every 15 min over 6 h (12 molar equiv relative to the substrate). The TLC separation was performed according to condition C.

Characterization Data for Acridine Derivatives. *1:2-Epoxy-1,2-dihydroacridine (**2**).* Yield (using condition A of the general procedure) 27% (15.8 mg); yellow amorphous solid; ^{1}H NMR ($CDCl_3$, 400 MHz) δ 4.15 (dt, ^3J = 3.6 Hz, ^4J = 1.6 Hz, 1H), 4.62 (d, ^3J = 3.6 Hz, 1H), 6.85 (dd, ^3J = 10.0 Hz, ^3J = 3.6 Hz, 1H), 7.01 (dd, ^3J = 10.0 Hz, ^4J = 1.6 Hz, 1H), 7.56 (ddd, ^3J = 8.0 Hz, ^3J = 6.8 Hz, ^4J = 1.2 Hz, 1H), 7.74 (ddd, ^3J = 8.4 Hz, ^3J = 6.8 Hz, ^4J = 1.6 Hz, 1H), 7.85 (dd, ^3J = 8.0 Hz, ^4J = 1.6 Hz, 1H), 8.09 (dd, ^3J = 8.4 Hz, ^3J = 1.2 Hz, 1H), 8.36 (s, 1H); ^{13}C{^{1}H} NMR (100 MHz, $CDCl_3$) δ 52.2, 56.4, 125.9, 127.2, 127.2, 127.5, 129.5, 130.4, 131.6, 134.2, 137.7, 148.3, 151.3; EI-MS *m/z* 195 ($M^{+\bullet}$), 179 ($M^{+\bullet}$ − O), 167 ($M^{+\bullet}$ − CO), 140 ($M^{+\bullet}$ − CO − C_2H_3); HRMS (ESI) *m/z* $[M + H]^+$ calcd for $C_{13}H_{10}NO$ 196.07624, found 196.07504.

*4-Hydroxyacridine (**3**).*[16] Yield (using condition A of the general procedure) 3% (1.8 mg); yellow amorphous solid; ^{1}H NMR ($CDCl_3$, 400 MHz) δ 7.20 (dd, ^3J = 7.2 Hz, ^4J = 1.2 Hz, 1H), 7.46 (dd, ^3J = 8.4 Hz, ^3J = 7.2 Hz, 1H), 7.53 (dd, ^3J = 8.4 Hz, ^4J = 1.2 Hz, 1H), 7.56 (ddd, ^3J = 8.4 Hz, ^3J = 6.4 Hz, ^4J = 0.8 Hz, 1H), 7.79 (ddd, ^3J = 8.8 Hz, ^3J = 6.4 Hz, ^3J = 1.2 Hz, 1H), 8.03 (d, ^3J = 8.4 Hz, 1H), 8.22 (d, ^3J = 8.8 Hz, 1H), 8.77 (s, 1H); ^{13}C{^{1}H} NMR (100 MHz, $CDCl_3$) δ 108.5, 118.3, 126.1, 126.8, 127.0, 127.5, 128.4, 129.2, 130.4, 136.2, 140.4, 147.1, 151.9; EI-MS *m/z* 195 ($M^{+\bullet}$), 167 ($M^{+\bullet}$ − CO), 140 ($M^{+\bullet}$ − CO − C_2H_3); HRMS (ESI) *m/z* $[M + H]^+$ calcd for $C_{13}H_{10}NO$ 196.07624, found 196.07422.

*anti-1:2,3:4-Diepoxy-1,2,3,4-tetrahydroacridine (**4**).* Yield (using condition B of the general procedure) 70% (44.4 mg); yellow amorphous solid; ^{1}H NMR ($CDCl_3$, 400 MHz) δ 3.95 (dd, ^3J = 4.0 Hz, ^4J = 0.8 Hz, 1H), 4.10 (d, ^3J = 4.0 Hz, 1H), 4.12 (m, 1H), 4.16 (m, 1H), 7.59 (ddd, ^3J = 8.0 Hz, ^3J = 6.8 Hz, ^4J = 1.2 Hz, 1H), 7.76 (ddd, ^3J = 8.4 Hz, ^3J = 6.8 Hz, ^4J = 1.6 Hz, 1H), 7.82 (d, ^3J = 8.0 Hz, 1H), 8.10 (d, ^3J = 8.4 Hz, 1H), 8.20 (s, 1H); ^{13}C{^{1}H} NMR (100 MHz, $CDCl_3$) δ 51.7, 54.1, 54.9, 55.9, 124.7, 127.5, 127.6, 127.9, 129.4, 130.7, 139.2, 147.9, 152.1; EI-MS *m/z* 211 ($M^{+\bullet}$), 182 ($M^{+\bullet}$ − CHO), 154 ($M^{+\bullet}$ − CHO − CO); HRMS (EI) *m/z* $M^{+\bullet}$ calcd for $C_{13}H_9NO_2$ 211.0633, found 211.0634.

*syn-1:2,3:4-Diepoxy-1,2,3,4-tetrahydroacridine (**5**).* Yield (using condition B of the general procedure) 17% (10.8 mg); yellow amorphous solid; ^{1}H NMR ($CDCl_3$, 400 MHz) δ 4.01 (t, ^3J = 3.2 Hz, 1H), 4.03 (t, ^3J = 3.2 Hz, 1H), 4.21 (d, ^3J = 3.2 Hz, 1H), 4.29 (d, ^3J = 3.2 Hz, 1H), 7.62 (ddd, ^3J = 8.0 Hz, ^3J = 6.8 Hz, ^4J = 1.2 Hz, 1H), 7.79 (ddd, ^3J = 8.4 Hz, ^3J = 6.8 Hz, ^4J = 1.6 Hz, 1H), 7.87 (d, ^3J = 8.0 Hz, 1H), 8.15 (d, ^3J = 8.4 Hz, 1H), 8.41 (s, 1H); ^{13}C{^{1}H} NMR (100 MHz, $CDCl_3$) δ 48.1, 48.6, 52.4, 52.5, 125.0, 127.6, 127.8, 127.9, 129.4, 130.8, 139.4, 148.0, 152.4; EI-MS *m/z* 211 ($M^{+\bullet}$), 182 ($M^{+\bullet}$ − CHO), 154 ($M^{+\bullet}$ − CHO − CO); HRMS (ESI) *m/z* $[M + H]^+$ calcd for $C_{13}H_{10}NO_2$ 212,07115, found 212.06965.

*1-Acetoxy-3:4-epoxy-2-hydroxy-1,2,3,4-tetrahydroacridine (**6**).* Yield (using condition C of the general procedure) 8% (6.5 mg); yellow amorphous solid; ^{1}H NMR ($CDCl_3$, 400 MHz) δ 2.07 (s, 3H), 3.99 (m, 1H), 4.34 (d, ^3J = 4.0 Hz, 1H), 4.65 (m, 1H), 6.10 (m, 1H), 7.54 (ddd, ^3J = 8.0 Hz, ^3J = 6.8 Hz, ^4J = 1.2 Hz, 1H), 7.72 (ddd, ^3J = 8.4 Hz, ^3J = 6.8 Hz, ^4J = 1.6 Hz, 1H), 7.72 (d, ^3J = 8.0 Hz, 1H), 8.06 (d, ^3J = 8.4 Hz, 1H), 8.18 (s, 1H); ^{13}C{^{1}H} NMR (100 MHz, $CDCl_3$) δ 21.4, 53.4, 56.6, 66.4, 72.3, 123.8, 127.4, 128.1, 128.2, 128.8, 130.8,

dx.doi.org/10.1021/jo5023525 | J. Org. Chem. 2015, 80, 281−289

141.1, 147.8, 153.3, 170.8; EI-MS m/z 271 ($M^{+\bullet}$), 228 ($M^{+\bullet} - CH_3CO$), 211 ($M^{+\bullet} - CH_3CO - OH$); HRMS (ESI) m/z $[M + H]^+$ calcd for $C_{13}H_{14}NO_4$ 272.09228, found 272.09046.

*3:4-Epoxy-1,2-dihydroxy-1,2,3,4-tetrahydroacridine (**7**).* Yield (using condition C of the general procedure) 11% (7.6 mg); yellow amorphous solid; ^{1}H NMR ($CDCl_3$, 400 MHz) δ 4.10 (ddd, ^3J = 4.0 Hz, ^3J = 2.4 Hz, ^4J = 2.4 Hz, 1H), 4.47 (d, ^3J = 4.0 Hz, 1H), 4.75 (m, 2H), 7.57 (ddd, ^3J = 8.0 Hz, ^3J = 6.8 Hz, ^4J = 1.2 Hz, 1H), 7.76 (ddd, ^3J = 8.4 Hz, ^3J = 6.8 Hz, ^4J = 1.6 Hz, 1H), 7.79 (d, ^3J = 8.0 Hz, 1H), 8.10 (d, ^3J = 8.4 Hz, 1H), 8.14 (s, 1H); ^{13}C{^{1}H} NMR (100 MHz, $CDCl_3$) δ 55.1, 57.7, 67.0, 72.6, 127.6, 128.0, 128.4, 128.5, 128.9, 130.6, 139.6, 147.7, 152.5; EI-MS m/z 229 ($M^{+\bullet}$), 200 ($M^{+\bullet} - COH$), 182 ($M^{+\bullet} - COH - H_2O$); HRMS (ESI) m/z $[M + H]^+$ calcd for $C_{13}H_{12}NO_3$ 230.08117, found 230.07954.

*anti,anti-1:2,3:4,5:6,7:8-Tetraepoxy-1,2,3,4,5,6,7,8-octahydroacridine (**8a**).* Yield (using condition C of the general procedure) 15% (10.9 mg); dark-yellow amorphous solid; ^{1}H NMR ($CDCl_3$, 400 MHz) δ 3.71 (dd, ^3J = 4.0 Hz, ^4J = 0.4 Hz, 2H), 3.89 (d, ^3J = 4.0 Hz, 2H), 4.04 (m, 2H), 4.07 (m, 2H), 7.76 (s, 1H); EI-MS m/z 243 ($M^{+\bullet}$), 214 ($M^{+\bullet} - COH$), 186 ($M^{+\bullet} - COH - CO$), 158 ($M^{+\bullet} - COH - 2CO$), 130 ($M^{+\bullet} - COH - 3CO$); HRMS (ESI) m/z $[M + H]^+$ calcd for $C_{13}H_{10}NO_4$ 244.06098, found 244.05923.

*anti,anti-1:2,3:4,5:6,7:8-Tetraepoxy-1,2,3,4,5,6,7,8-tetrahydroacridine (**8b**).* Yield (using condition C of the general procedure) 6% (4.4 mg); dark-yellow amorphous solid; ^{1}H NMR ($CDCl_3$, 400 MHz) δ 3.72 (dd, ^3J = 3.6 Hz, ^4J = 0.4 Hz, 2H), 3.90 (d, ^3J = 4.0 Hz, 2H), 4.04 (m, 2H), 4.07 (m, 2H), 7.75 (s, 1H); EI-MS m/z 243 ($M^{+\bullet}$), 214 ($M^{+\bullet} - COH$), 186 ($M^{+\bullet} - COH - CO$), 158 ($M^{+\bullet} - COH - 2CO$), 130 ($M^{+\bullet} - COH - 3CO$); HRMS (ESI) m/z $[M + H]^+$ calcd for $C_{13}H_{10}NO_4$ 244.06098, found 244.05923.

Reaction of Compound 4 with 4-Ethylaniline in a Microwave Reactor. In a 10 mL vessel, **4** and 4-ethylaniline were dissolved in 6 mL of acetonitrile in equivalent amounts. The vessel was placed in the cavity of a microwave reactor, and the reaction mixture was irradiated at 80 °C for 10 min using a maximum power of 150 W. At the end of the reaction, the solvent was evaporated, and the final residue was dissolved in $CDCl_3$ to be analyzed by ^{1}H NMR spectroscopy.

*1-(4′-Ethylphenylamino)-3:4-epoxy-2-hydroxy-1,2,3,4-tetrahydroacridine (**9**).* ^{1}H NMR ($CDCl_3$, 400 MHz) δ 1.18 (t, ^3J = 7.6 Hz, 3H, $-CH_3$), 2.54 (q, ^3J = 7.6 Hz, 2H, $-CH_2-$), 3.31 (br s, 1H, NH), 4.00 (m, 1H, H3), 4.33 (d, ^3J = 4.0 Hz, 1H, H4), 4.72 (m, 1H, H2), 4.81 (m, 1H, H1), 6.64 (m, 2H, H3′, H5′), 7.00 (m, 2H, H2′, H6′), 7.41 (ddd, ^3J = 8.0 Hz, ^3J = 6.8 Hz, ^4J = 1.2 Hz, 1H, H7), 7.50 (d, ^3J = 8.0 Hz, 1H, H8), 7.63 (ddd, ^3J = 8.4 Hz, ^3J = 6.8 Hz, ^4J = 1.6 Hz, 1H, H6), 7.82 (s, 1H, H9), 7.95 (d, ^3J = 8.4 Hz, 1H, H5). ^{13}C NMR (100 MHz, $CDCl_3$) δ 16.0 ($-CH_3$), 28.0 ($-CH_2-$), 54.4 (C4), 57.8 (C1), 58.1 (C3), 66.1 (C2), 114.6 (C2′, C6′), 127.0 (C7), 127.9 (C9a), 127.9 (C8), 128.2 (C8a), 128.4 (C5), 128.9 (C3′, C5′), 129.9 (C6), 134.5 (C4′), 138.4 (C9), 144.0 (C1′), 147.1 (C10a), 152.7 (C4a).

Computational Studies. DFT calculations were carried out using Gaussian 09.[37] Geometry optimizations were performed at the B3LYP/6-31G(d,p)/B3LYP/6-311++G(d,p) level of theory.[38−41] The effect of the solvent was simulated using the polarizable continuum model (IEF-PCM).[42] Graphical representations of the optimized structures were produced with the GaussView molecular visualization program.[43] After optimization, ^{1}H NMR chemical shifts were calculated using the gauge-independent atomic orbital (GIAO) method[44,45] in chloroform at the B3LYP/6-311++G(d,p) level under the keyword NMR = MIXED. Chemical shifts are reported in parts per million relative to tetramethylsilane (TMS) calculated at the same level of theory. The calculated ^{1}H and ^{13}C isotropic chemical shieldings for TMS in chloroform at the same level of theory were 32 and 184.8 ppm, respectively.

Acridine (**1**) was used as a reference in the DFT calculations in which comparisons between theoretical and experimental values of the chemical shifts in the ^{1}H NMR spectrum of acridine were performed. The mean absolute error, denoted as $\overline{|\Delta\delta|}$, was calculated using the formula

$$\overline{|\Delta\delta|} = \frac{1}{n}\sum_{i=1}^{n}|\delta_{\text{theoretical},i} - \delta_{\text{experimental},i}| = \frac{1}{n}\sum_{i=1}^{n}|\Delta\delta_i| \quad (1)$$

Then the mean absolute deviation, denoted as $\bar{\mathbf{D}}$, was calculated using the formula

$$\bar{\mathbf{D}} = \frac{1}{n}\sum_{i=1}^{n}||\Delta\delta_i| - \overline{|\Delta\delta|}| \quad (2)$$

The values of $\bar{\mathbf{D}}$ obtained for the ^{1}H and ^{13}C NMR chemical shifts of acridine were 0.03 and 0.4, respectively (see the Supporting Information). These values were used as references for the subsequent studies to reach reliable conclusions from the comparisons between experimental and theoretical ^{1}H and ^{13}C NMR shifts, respectively.

■ ASSOCIATED CONTENT

Ⓢ Supporting Information

The structure of the catalyst; characterization data for compounds; ^{1}H and ^{13}C NMR spectra; 2D NMR spectra; EI mass spectra and ESI exact mass spectra; ^{1}H NMR spectrum of the total reaction mixture; complementary DFT-optimized structures and ESP maps; geometric parameters; and tables of comparison of experimental with computational data. This material is available free of charge via the Internet at http://pubs.acs.org.

■ AUTHOR INFORMATION

Corresponding Author

*E-mail: susana.rebelo@fc.up.pt.

Notes

The authors declare no competing financial interest.

■ ACKNOWLEDGMENTS

This work was funded by Fundação para a Ciência e a Tecnologia (FCT, Portugal), and FEDER through Grants PEst-C/EQB/LA0006/2013, FCOMP-01-0124-FEDER-037285, and NORTE-07-0124-FEDER-000067-Nanochemistry. The NMR spectra were acquired at CEMUP at the University of Porto, funded by the Portuguese National NMR Network.

■ REFERENCES

(1) Mitra, P.; Chakraborty, P. K.; Saha, P.; Ray, P.; Basu, S. *Int. J. Pharm.* **2014**, *473*, 636.

(2) Zawada, Z.; Šafařík, M.; Dvořáková, E.; Janoušková, O.; Březinová, A.; Stibor, I.; Holada, K.; Bouř, P.; Hlaváček, J.; Sebestík, J. *Amino Acids* **2013**, *44*, 1279.

(3) Belmont, P.; Bosson, J.; Godet, T.; Tiano, M. *Anti-Cancer Agents Med. Chem.* **2007**, *7*, 139.

(4) Denny, W. A. *Curr. Med. Chem.* **2002**, *9*, 1655.

(5) Cholewiński, G.; Dzierzbicka, K.; Kołodziejczyk, A. M. *Pharmacol. Rep.* **2011**, *63*, 305.

(6) Zhang, B.; Li, X.; Li, B.; Gao, C.; Jiang, Y. *Expert Opin. Ther. Patents* **2014**, *24*, 647.

(7) Ferguson, L. R.; Denny, W. A. *Mutat. Res.* **1991**, *258*, 123.

(8) Chen, Y. Y.; Lukka, P. B.; Joseph, W. R.; Finlay, G. J.; Paxton, J. W.; McKeage, M. J.; Baguley, B. C. *Cancer Chemother. Pharmacol.* **2014**, *74*, 25.

(9) Benoit, A. R.; Schiaffo, C.; Salomon, C. E.; Goodell, J. R.; Hiasa, H.; Ferguson, D. M. *Bioorg. Med. Chem. Lett.* **2014**, *24*, 3014.

(10) Bierbach, U.; Suryadi, J. *Chem.—Eur. J.* **2012**, *18*, 12926.

(11) Murray, V.; Chen, J. K.; Galea, A. M. *Anti-Cancer Agents Med. Chem.* **2014**, *5*, 695.

(12) Martí-Centelles, V.; Burguete, M. I.; Galindo, F.; Izquierdo, M. A.; Kumar, D. K.; White, A. J. P.; Luis, S. V.; Vilar, R. *J. Org. Chem.* **2012**, *77*, 490.

(13) Krzymiński, K.; Ożóg, A.; Malecha, P.; Roshal, A. D.; Wróblewska, A.; Zadykowicz, B.; Bzażejowski, J. *J. Org. Chem.* **2011**, *76*, 1072.
(14) Li, Q.; Xu, K.; Song, P.; Dai, Y.; Yang, L.; Pang, X. *Dyes Pigm.* **2014**, *109*, 169.
(15) Acheson, R. M. *The Chemistry of Heterocyclic Compounds: Acridines*; Wiley: New York, 1973.
(16) Bos, R.; Barnett, N. W.; Dyson, G. A.; Russell, R. A. *Anal. Chim. Acta* **2002**, *454*, 147.
(17) *Cytochrome P450: Structure, Mechanism, and Biochemistry*, 3rd ed.; Ortiz de Montellano, P. R., Ed.; Plenum Publishing: New York, 2005.
(18) Marchetti, L.; Levine, M. *ACS Catal.* **2011**, *1*, 1090.
(19) *Biochemistry and Binding: Activation of Small Molecules*; Kadish, K. M., Smith, K. M., Guilard, R., Eds.; The Porphyrin Handbook, Vol. *4*; Academic Press: New York, 2000.
(20) Roat-Malone, R. M. *Bioinorganic Chemistry: A Short Course*; Wiley: New York, 2003.
(21) Lanza, D. L.; Code, E.; Crespi, C. L.; Gonzalez, F. J.; Yost, G. S. *Drug Metab. Dispos.* **1999**, *27*, 798.
(22) Hao, W.-J.; Wang, J.-Q.; Xu, X.-P.; Zhang, S.-L.; Wang, S.-Y.; Ji, S.-J. *J. Org. Chem.* **2013**, *78*, 12362.
(23) Verma, A. K.; Kotla, S. K. R.; Aggarwal, T.; Kumar, S.; Nimesh, H.; Tiwari, R. K. *J. Org. Chem.* **2013**, *78*, 5372.
(24) Lipińska, M. E.; Rebelo, S. L. H.; Freire, C. *J. Mater. Sci.* **2014**, *49*, 1494.
(25) Rebelo, S. L. H.; Pereira, M. M.; Monsanto, P. V.; Burrows, H. D. *J. Mol. Catal. A: Chem.* **2009**, *297*, 35.
(26) Pires, S. M. G.; Simões, M. M. Q.; Santos, I. C. M. S.; Rebelo, S. L. H.; Pereira, M. M.; Neves, M. G. P. M. S.; Cavaleiro, J. A. S. *Appl. Catal., A* **2012**, *439*−*440*, 51.
(27) Pires, S. M. G.; Simões, M. M. Q.; Santos, I. C. M. S.; Rebelo, S. L. H.; Paz, F. A. A.; Neves, M. G. P. M. S.; Cavaleiro, J. A. S. *Appl. Catal., B* **2014**, *160*−*161*, 80.
(28) da Silva, G.; Pires, S. M. G.; Silva, V. L. M.; Simões, M. M. Q.; Neves, M. G. P. M. S.; Rebelo, S. L. H.; Silva, A. M. S.; Cavaleiro, J. A. S *Catal. Commun.* **2014**, *56*, 68.
(29) Linhares, M.; Rebelo, S. L. H.; Simões, M. M. Q.; Silva, A. M. S.; Neves, M. G. P. M. S.; Cavaleiro, J. A. S.; Freire, C. *Appl. Catal., A* **2014**, *470*, 427.
(30) Costa, P.; Linhares, M.; Rebelo, S. L. H.; Neves, M. G. P. M. S.; Freire, C. *RSC Adv.* **2013**, *3*, 5350.
(31) Rocha, M.; Rebelo, S. L. H.; Freire, C. *Appl. Catal., A* **2013**, *460*−*461*, 116.
(32) Li, J.-L.; Zhang, X.; Huang, X.-R. *Phys. Chem. Chem. Phys.* **2012**, *14*, 246−256.
(33) Jerina, D. M.; Daly, J. W. *Science* **1974**, *185*, 573.
(34) Kang, M.-J.; Song, W. J.; Han, A.-R.; Choi, Y. S.; Jang, H. G.; Nam, W. *J. Org. Chem.* **2007**, *72*, 6301.
(35) Thibon, A.; Jollet, V.; Ribal, C.; Sénéchal-David, K.; Billon, L.; Sorokin, A. B.; Banse, F. *Chem.—Eur. J.* **2012**, *18*, 2715.
(36) Rebelo, S. L. H.; Linhares, M.; Simões, M. M. Q.; Silva, A. M. S.; Neves, M. G. P. M. S.; Cavaleiro, J. A. S.; Freire, C. *J. Catal.* **2014**, *315*, 33.
(37) Frisch, M. J.; Trucks, G. W.; Schlegel, H. B.; Scuseria, G. E.; Robb, M. A.; Cheeseman, J. R.; Scalmani, G.; Barone, V.; Mennucci, B.; Petersson, G. A.; Nakatsuji, H.; Caricato, M.; Li, X.; Hratchian, H. P.; Izmaylov, A. F.; Bloino, J.; Zheng, G.; Sonnenberg, J. L.; Hada, M.; Ehara, M.; Toyota, K.; Fukuda, R.; Hasegawa, J.; Ishida, M.; Nakajima, T.; Honda, Y.; Kitao, O.; Nakai, H.; Vreven, T.; Montgomery, J. A., Jr.; Peralta, J. E.; Ogliaro, F.; Bearpark, M.; Heyd, J. J.; Brothers, E.; Kudin, K. N.; Staroverov, V. N.; Kobayashi, R.; Normand, J.; Raghavachari, K.; Rendell, A.; Burant, J. C.; Iyengar, S. S.; Tomasi, J.; Cossi, M.; Rega, N.; Millam, J. M.; Klene, M.; Knox, J. E.; Cross, J. B.; Bakken, V.; Adamo, C.; Jaramillo, J.; Gomperts, R.; Stratmann, R. E.; Yazyev, O.; Austin, A. J.; Cammi, R.; Pomelli, C.; Ochterski, J. W.; Martin, R. L.; Morokuma, K.; Zakrzewski, V. G.; Voth, G. A.; Salvador, P.; Dannenberg, J. J.; Dapprich, S.; Daniels, A. D.; Farkas, Ö.; Foresman, J. B.; Ortiz, J. V.; Cioslowski, J.; Fox, D. J. *Gaussian 09*, revision A.1; Gaussian, Inc.: Wallingford, CT, 2009.
(38) Becke, A. D. *J. Chem. Phys.* **1993**, *98*, 5648.
(39) Becke, A. D. *Phys. Rev. A* **1988**, *38*, 3098.
(40) Lee, C.; Yang, W.; Parr, R. G. *Phys. Rev. B* **1988**, *37*, 785.
(41) Stevens, P. J.; Devlin, F. J.; Chabalowski, C. F.; Frisch, M. J. *J. Chem. Phys.* **1994**, *98*, 11623.
(42) Mennucci, B.; Cancès, E.; Tomasi, J. *J. Phys. Chem. B* **1997**, *101*, 10506.
(43) Dennington, R.; Keith, T.; Millam, J. *GaussView*, version 5; Semichem Inc.: Shawnee Mission, KS, 2009.
(44) Ditchfield, R. *Mol. Phys.* **1974**, *27*, 789.
(45) Wolinski, K.; Hilton, J. F.; Pulay, P. *J. Am. Chem. Soc.* **1990**, *112*, 8251.